Novel lithium-loaded porous aromatic framework for efficient CO2 and H2 uptake

ARTICLE · DECEMBER 2012

DOI: 10.1039/C2TA00616B

8 AUTHORS, INCLUDING:

Ma Heping
Jilin University
19 PUBLICATIONS **269** CITATIONS
SEE PROFILE

Xiaoqin Zou
Jilin University
30 PUBLICATIONS **574** CITATIONS
SEE PROFILE

Fu Xing Sun
Jilin University
75 PUBLICATIONS **1,715** CITATIONS
SEE PROFILE

Journal of Materials Chemistry A

RSC Publishing

PAPER

View Article Online
View Journal | View Issue

Novel lithium-loaded porous aromatic framework for efficient CO_2 and H_2 uptake†

Cite this: *J. Mater. Chem. A*, 2013, **1**, 752

Heping Ma,[a] Hao Ren,[a] Xiaoqin Zou,[a] Fuxing Sun,[a] Zhuojun Yan,[a] Kun Cai,[a] Dayang Wang[b] and Guangshan Zhu*[ac]

Received 9th October 2012
Accepted 17th October 2012

DOI: 10.1039/c2ta00616b

www.rsc.org/MaterialsA

Novel porous aromatic frameworks, PAF-18-OH and its lithiated derivative PAF-18-OLi, have been successfully synthesized. In particular, PAF-18-OLi displays significant enhancement of H_2 and CO_2 adsorption capacity, especially for CO_2 uptake (14.4 wt%). More valuably, the stable PAF-18-OLi material exhibits high CO_2/N_2 selectivity, as high as 129 in the case of CO_2 capture from simulated post-combustion flue gas mixtures (85% N_2 and 15% CO_2). Furthermore, the PAF-18-OLi has shown improved H_2 storage capacity after lithiation.

Introduction

Environmental degeneration and adverse climate change are currently two of the challenges most affecting our daily life.[1] The increasing utilization of world's fast diminishing fossil fuels is a major source of environmental pollution.[2] The emission of CO_2 is considered as the most significant contribution to global warming among all of the Earth's radiative-forcing components.[3] To solve these two pressing environmental issues, it requires the development of new technologies for capture and sequestration of CO_2 and to efficiently harness a range of renewable energy sources and carriers such as H_2.[4] Porous materials, such as activated carbon,[5] zeolites,[6] and metal–organic frameworks (MOFs),[7] have demonstrated promising prospects in applications for H_2 storage and CO_2 capture owing to their high specific surface areas and low energy consumption for regeneration. Recently, a new family of porous materials, porous organic frameworks (POFs), composed of light elements (C, H, O, N, B, *etc.*) *via* covalent bonds, have attracted a great deal of attention thanks to their high surface areas, high stability and controllable skeletons.[8–13] Current investigations have demonstrated that POFs are promising materials for H_2 storage and CO_2 capture.[14]

To date, H_2 storage in porous materials is usually implemented under either high pressure or very low temperature conditions, which are not easily adapted in commercial and realistic applications.[2a] Traditional CO_2 capture is based on the chemical absorption of CO_2 using aqueous solutions of amines,[15] and a substantially large amount of energy is required for activity regeneration of the amines. Although the use of porous materials for physical adsorption of CO_2 is fairly energy-effective, a considerable amount of N_2 is co-adsorbed in the porous materials, resulting in low CO_2/N_2 selectivity.[16] To enhance H_2 or CO_2 uptake and especially to improve the CO_2/N_2 adsorption selectivity, porous materials should possess strong interactions with H_2 or CO_2. Several strategies in the literature have been developed to enhance the interactions between porous materials and gas molecules *via* the control of the pore size, incorporation of polar functional groups or the introduction of open metal sites into the porous networks.[17] For instance, doping atomically dispersed alkali metal cations, for example Li^+ ions, into MOFs and POFs is expected to increase their H_2 and CO_2 storage capacities.[18,19a] However, Li^+-doped MOFs or POFs have limited success in H_2 storage and CO_2 capture due to the instability of Li^+ ions or the modified porous structures.[19] Herein, we synthesized new porous aromatic frameworks (PAFs) with permanent porosity and functionalized OH groups, referred to as PAF-18-OH. The OH groups of PAF-18-OH have been further transformed into lithium alkoxy groups, resulting in lithium-loaded PAF, referred to as PAF-18-OLi (Scheme 1).

PAF-18-OLi has exhibited a significantly increased uptake of CO_2 with high CO_2/N_2 selectivity as large as 129 at 273 K. Furthermore, the PAF-18-OLi has shown enhanced H_2 storage capacity.

Experimental section

Chemicals

All chemicals were purchased from Aldrich, Alfa-Aesar, and Aladdin-Reagent, and used as received unless it was noted.

[a]*State Key Laboratory of Inorganic Synthesis & Preparative Chemistry, Jilin University, Changchun, 130012, China. E-mail: zhugs@jlu.edu.cn; Fax: +86 431-8516-8331*

[b]*Ian Wark Research Institute, University of South Australia, Mawson Lakes Campus, Adelaide, SA 5095, Australia*

[c]*Queensland Micro- and Nanotechnology Centre, Griffith University, Queensland, 4111, Australia*

† Electronic supplementary information (ESI) available: This material includes: XRD, SEM, IR, TG, XPS figures; CO_2 and H_2 adsorption isotherms of PAF-18-OLi with different Li contents as well as details on the calculations of Q_{st} and selectivity from ideal adsorption solution theory (IAST). See DOI: 10.1039/c2ta00616b

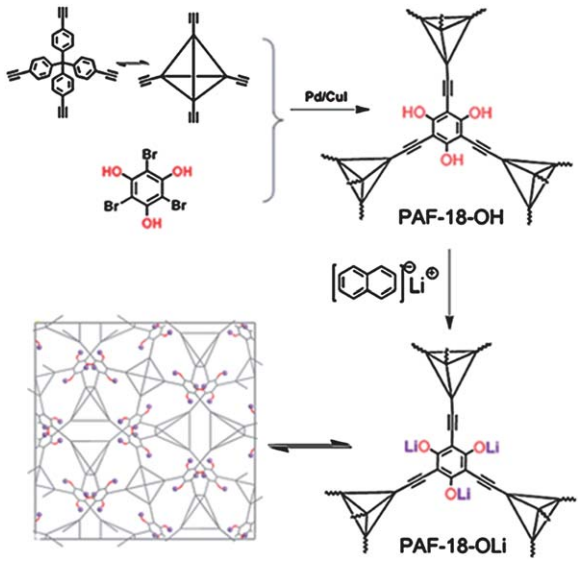

Scheme 1 Schematic depiction of the synthesis of PAF-18-OH and PAF-18-OLi.

N,*N*-Dimethylformamide (DMF) and triethylamine (Et_3N) were dehydrated with CaH_2. Tetrahydrofuran (THF) was distilled in the presence of sodium benzophenone ketyl under N_2 conditions. Tetrakis(4-ethynylphenyl)methane[20a] and 2,4,6-tribromobenzene-1,3,5-triol[20b] were prepared according to the previously reported methods.

Synthesis of PAF-18-OH

Tetrakis(4-ethynylphenyl)methane (125 mg, 1.5 mmol), 2,4,6-tribromo-benzene-1,3,5-triol (116 mg, 1.5 mmol), tetrakis-(triphenphosphine)palladium (30 mg), and copper iodide (8 mg) were dissolved in a mixture of DMF (5 mL) and Et_3N (5 mL) in a 50 mL two-necked flask. After degassing *via* three freeze–pump–thaw cycles, the mixture was stirred at 85 °C for 36 h under N_2. After cooling down to room temperature, the resulting PAF-18-OH was collected by filtration, followed by consecutive washing by Soxhlet extraction for 48 h with THF, methanol to remove the unreacted monomers or catalysts. After drying at 90 °C in vacuum overnight, PAF-18-OH was obtained in the form of a brown powder (150 mg, 90% yield).

Synthesis of PAF-18-OLi

Synthesis of PAF-18-OLi was performed in an argon atmosphere glove box. Lithium-naphthalenide ($Li^+C_{10}H_8^-$) was synthesized by adding small pieces of clean lithium (3 mg, stored in glove box) into 100 mL naphthalene solution in THF (0.1 M), followed by 4 h vigorous stirring. After reaction, the solution became dark green; a given volume of this solution was taken out using a volumetric syringe and mixed with dried powders of PAF-18-OH with a given mass (see ESI†). After stirring overnight to ensure the complete reaction of $Li^+C_{10}H_8^-$ with PAF-18-OH, the powder of PAF-18-OLi was filtrated and washed with THF several times to remove naphthalene and then dried under vacuum at 120 °C for 12 h.

Characterization

FTIR spectra were obtained using an IFS 66V/S Fourier transform infrared spectrometer. Thermogravimetric analysis (TG) was implemented using a Netzch Sta 449c thermal analyzer system at a heating rate of 10 °C min^{-1} under air. Scanning electron microscopy (SEM) imaging was performed on a JEOS JSM 6700. Transmission electron microscopy (TEM) imaging was carried out on a JEOL JEM 3010 with an acceleration voltage of 300 kV. X-ray photoelectron spectroscopy (XPS, ESCALAB 250, Thermo Scientific) was performed by using a monochromatized Al Kα (1486.6 eV) X-ray source. ^{7}Li MAS NMR spectra were recorded on a Bruker AVANCE III 400 WB spectrometer. Powder X-ray diffraction (PXRD) was carried out by a Riguku D/MAX2550 diffractometer using CuKα radiation, 40 kV, 200 mA with a scanning rate of 3° min^{-1} (2θ). The lithium content in PAF-18-OLi was determined by inductively coupled plasma (ICP) spectroscopy (Perkin-Elmer ICP-OES Optima 3300DV). Before analysis, ~15 mg of sample was digested in 3 : 1 HCl–HNO_3 (10 mL) and transferred to a 50 mL volumetric flask with distilled water.

Low-pressure gas adsorption measurements

The gas adsorption–desorption isotherms were measured on a Quantachrome Autosorb iQ2 analyzer. N_2 adsorption–desorption measurements were carried out at 77 K, 273 K, and 298 K; H_2 adsorption–desorption isotherms were recorded at 77 K and 87 K, and CO_2 adsorption–desorption isotherms were collected at 273 K and 298 K, respectively. Ultra-high-purity grade (99.99%) N_2, H_2, and CO_2 gases were used for all adsorption measurements. Liquid nitrogen and liquid argon baths were utilized to control the temperature at 77 K and 87 K, respectively. An ice-water bath and water baths equipped with a temperature sensor were used to control the temperature at 273 K and 298 K.

Results and discussion

Description of PAF-18-OH and PAF-18-OLi

PAF-18-OH was synthesized *via* the palladium-catalyzed Sonogashira–Hagihara cross-coupling reaction of tetrahedral tetrakis(4-ethynylphenyl)methane (TEPM) and planar triangular unit 2,4,6-tribromo-benzene-1,3,5-triol (TBBT).[21] The resulted product is characterized by PXRD, and the XRD pattern shows that the product is in amorphous phase (Fig. S1†). The ^{13}C CP-MAS NMR spectrum confirms the successful synthesis of PAF-18-OH with characteristic peaks from the joint monomers (Fig. S2†). The FT-IR spectra of the as-prepared PAF-18-OH clearly indicate the presence of OH groups (Fig. S3a†). The thermogravimetric analysis (TG) shows the decomposition of PAF-18-OH starts at a temperature of 350 °C under air (Fig. S4†), suggesting this material possesses excellent thermal stability. The PAF-18-OH is insoluble in common organic solvents, such as THF, acetone, ethanol, DMF, and DMSO, indicating high chemical stability.

After reaction with lithium naphthalenide ($Li^+C_{10}H_8^-$ in THF),[22] the protons of PAF-18-OH are replaced by Li ions,

yielding PAF-18-OLi. The complete lithiation of PAF-18-OH has been confirmed by the disappearance of the OH stretching vibration band centered at 3432 cm^{-1} in the FT-IR spectrum of PAF-18-OLi (Fig. S3b†). The Li content of PAF-18-OLi could be readily tuned by altering the molar ratio of $Li^+C_{10}H_8^-$ to the OH groups of PAF-18-OH. In our work, the complete lithation yields a maximum Li content of 4.2 wt% in the resulting PAF-18-OLi, very close to the theoretical value, 4.5 wt%. The high-resolution XPS (Fig. S5†) and ^{7}Li MAS NMR spectroscopy (Fig. S6†) analyses of PAF-18-OLi indicate that Li is present in the ionic state in high-purity PAF material.[23]

Furthermore, the morphologies of PAF-18-OH and its derivative PAF-18-OLi are monitored by scanning electron microscopy (SEM). The SEM images show that both PAF-18-OH and PAF-18-OLi are aggregates of microgel particles with a size of 100 nm (Fig. 1a and b). The appearance of PAF-18-OLi is similar to PAF-18-OH, indicating that the structure of PAF-18-OLi is preserved after lithiation. In addition, the microstructure is studied by transmission electron microscopy (TEM). The TEM images of PAF-18-OH and PAF-18-OLi are displayed in Fig. 1c and d. As can be seen, a worm-like porous texture is observed in both materials.

Porosity of PAF-18-OH and PAF-18-OLi

The porosity of PAF-18-OH and PAF-18-OLi is probed by physical nitrogen sorption at 77 K. A sharp increase in gas uptake is observed at low pressure in the nitrogen adsorption–desorption isotherms of PAF-18-OH and PAF-18-OLi, which further confirms the existence of micropores in both PAFs; a distinct adsorption–desorption hysteresis at high relative pressure sheds light on the presence of some mesopores, which is a common characteristic for many porous organic frameworks (Fig. 2a).[24,18c]

The Brunauer–Emmett–Teller (BET) surface area of PAF-18-OH is measured as 1121 m^2 g^{-1}. As shown in Fig. 2a, the lithiation of PAF-18-OH causes a small reduction in the BET surface area. The BET surface areas of PAF-18-OLi are decreasing with increasing lithium content. Typically, a surface area of 981 m^2 g^{-1} is obtained after complete lithation (Li content is 4.2 wt%) (Table S1†). The pore size distributions of PAF-18-OH and PAF-18-OLi have been calculated based on non-local density functional theory. As shown in Fig. 2b, the transformation of the OH groups into lithium alkoxy groups gives negligible change in the pore size distribution within the PAF-18 materials (Table 1). The small change in pore width is interpreted to be from the very close radii of ionic lithium and the hydrogen atom. However, an increase of the density after lithiation causes a noticeable decrease in the pore volume (Fig. 2c), which is the same phenomenon observed from the small reduction of the surface areas of the PAFs. The calculated pore volumes for PAF-18-OH and PAF-18-OLi are 0.82 and 0.57 cm^3 g^{-1}, respectively. Also, PAF-18-OLi exhibits a micropore volume of 0.34 cm^3 g^{-1}, which is a bit less than that of PAF-18-OH (0.4 cm^3 g^{-1}).

The CO_2 adsorption for PAF-18-OH and PAF-18-OLi

Given the particular polarity of PAF-18-OH and PAF-18-OLi for effective adsorption of CO_2,[17] the –OLi in PAFs may provide strong polar open coordination sites, which could result in stronger interactions with CO_2 molecules. The CO_2 adsorption is studied on both PAF-18-OH and PAF-18-OLi samples (Fig. 3).

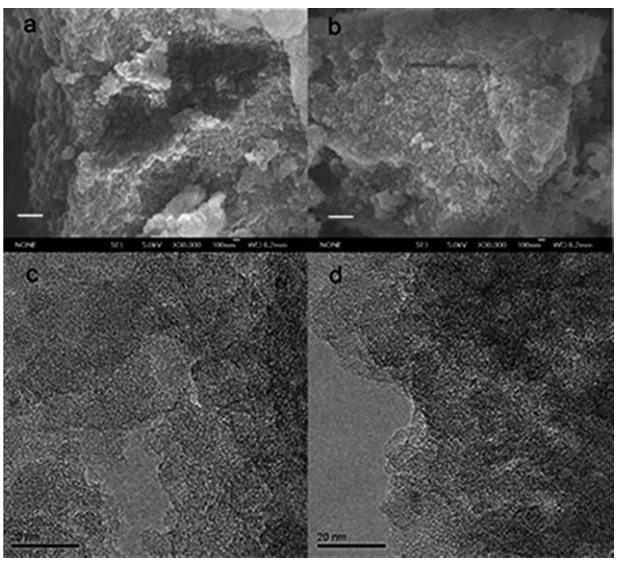

Fig. 1 SEM images of PAF-18-OH (a), PAF-18-OLi (b), scale bars: 300 nm. TEM images of PAF-18-OH (c), PAF-18-OLi (d), scale bars: 20 nm.

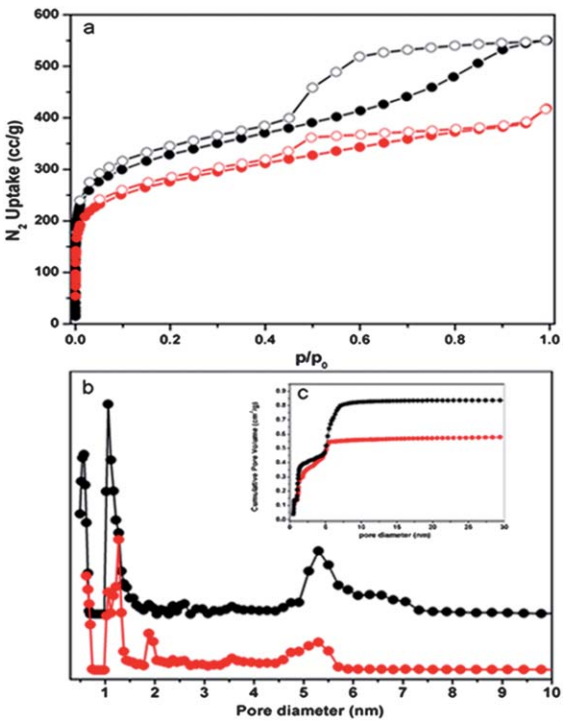

Fig. 2 (a) N_2 adsorption (solid circles) and desorption (open circles) isotherms of PAF-18-OH (black symbols) and PAF-18-OLi (red symbols) at 77 K; (b) the pore size distribution of PAF-18-OH (black circles) and PAF-18-OLi (red circles), (c) the corresponding cumulative pore volume distributions are shown in the inset.

Table 1 The properties of porosity, gas uptake and isosteric heat of adsorption of PAF-18-OH and PAF-18-OLi

Materials	BET (m^2 g^{-1})	DFT pore diameter (nm)	Total pore volume (cm^3 g^{-1})	Micropore volume (cm^3 g^{-1})	CO_2 uptake 273 K (wt%)	Q_{st} for CO_2 (kJ mol^{-1})	H_2 uptake 77 K (wt%)	Q_{st} for H_2 (kJ mol^{-1})
PAF-18-OH	1121	1.33	0.82	0.4	11	28	1.35	7.4
PAF-18-OLi	981	1.32	0.57	0.34	14.4	29.5	1.65	7.6

Fig. 3a shows that the CO_2 uptake of PAF-18-OH is about 110 mg g^{-1} at 273 K, and 66 mg g^{-1} at 298 K at 1 bar, respectively. The PAF-18-OLi with 4.2 wt% Li shows a maximum CO_2 uptake; 144 mg g^{-1} at 273 K, and 89 mg g^{-1} at 298 K at 1 bar, respectively, which are comparable to the best CO_2 adsorption performances of lithiated MOFs and POFs reported in the open literature.[25] Additionally, in the case of PAF-18-OLi, the CO_2 uptake is increasing with more Li content introduced into the PAF structure (Fig. S7a†). When the Li content is larger than 4.2 wt%, the CO_2 uptake decreases distinctly. Excess lithium would aggregate on the skeleton surface, which poses a negative contribution to CO_2 uptake.

The affinity of guest molecules to host materials is usually evaluated by the isosteric heat of adsorption (Q_{st}).[26] Fig. 3b shows that PAF-18-OLi has a larger Q_{st} than that of PAF-18-OH; the Q_{st} value of PAF-18-OLi is slowly reduced from 29.5 kJ mol^{-1} to 23.5 kJ mol^{-1} as the CO_2 uptake reaches the maximum, while the Q_{st} of PAF-18-OH goes from 28 kJ mol^{-1} to 23 kJ mol^{-1} (details of Q_{st} calculation in ESI†). Since the lithiation causes a reduction in the surface area and pore volume, the enhanced CO_2 uptake (Fig. 3a) could be assigned to the presence of the Li ions in the PAF-18-OLi framework. It is usually envisioned that the Li ions in PAF-18-OLi create a high electric field on the framework surface, which leads to a high binding force with quadrupolar CO_2 molecules.[27] Due to the high activity of Li ions, Li doped MOFs and POFs are usually unstable under wet conditions.[19b,c,e] To verify their stability under wet conditions, PAF-18-OLi samples were exposed to wet air (the average relative humidity is about 65%) for 10 days. This treatment causes little reduction in the CO_2 uptake of the PAF-18-OLi, as shown in Fig. 3a. This promises great potential for future application of PAF-18-OLi in rigorous conditions, such as in wet and under oxygen.

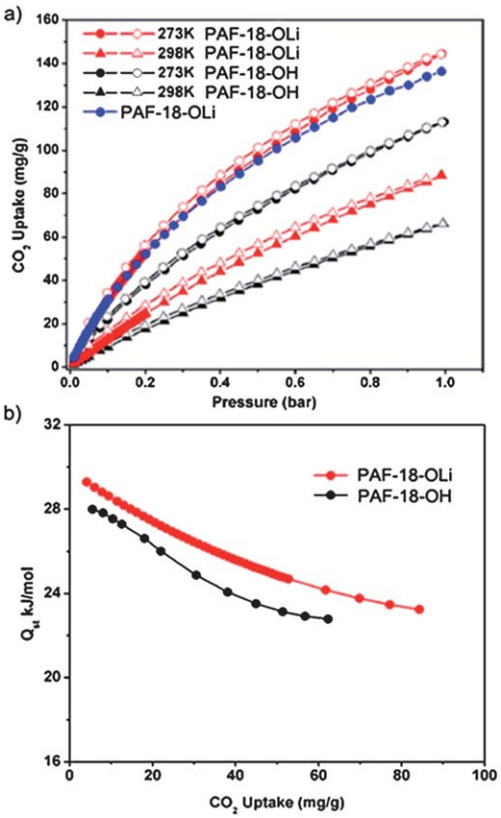

Fig. 3 (a) CO_2 adsorption (solid symbols) and desorption (open symbols) isotherms of PAF-18-OH and PAF-18-OLi at 273 K and 298 K. CO_2 adsorption of PAF-18-OLi obtained after 10 days exposure in wet air (blue circles) at 273 K. (b) Plots of the isosteric heat of adsorption (Q_{st}) for CO_2 of PAF-18-OH and PAF-18-OLi *versus* CO_2 uptake.

The CO_2/N_2 selectivities of PAF-18-OH and PAF-18-OLi

Carbon dioxide capture or storage from flue gas (>70% N_2 content) is critical to reduce the global greenhouse effect.[4] On the other hand, CO_2 is a useful chemical raw resource in industry. From the environmental and energy perspective views, it requires adsorbents with large CO_2 adsorption capacity but with low N_2 adsorption ability in the range of low pressure and at ambient temperature. The adsorption isotherms of PAF-18-OH and PAF-18-OLi for CO_2 are investigated at different temperatures of 273 K and 298 K, and the results are shown in Fig. 4. It is found that both PAF-18-OH and PAF-18-OLi exhibit pronounced CO_2 uptake and fairly low N_2 adsorption at a pressure <1 bar. The different adsorption ability towards CO_2 and N_2 provides a basis for the selective capture of CO_2 from gas mixture streams. We have employed the ideal adsorption solution theory (IAST) to assess the merits of lithiation for CO_2/N_2 separation, the method of which has been documented to accurately predict binary gas mixture adsorption in many porous materials.[28]

The dual-site Langmuir–Freundlich equation is used to fit the experimental single component adsorption isotherm. The selectivities of PAF-18-OH and PAF-18-OLi for CO_2 over N_2 in a post-combustion flue gas stream (typically 15% CO_2 and 85% N_2) are shown in Fig. 5. The CO_2/N_2 selectivity is 34 for PAF-18-OH and 129 for PAF-18-OLi at 273 K, respectively. After the temperature is elevated from 273 K to 298 K, the selectivities are correspondingly reduced to 16 for PAF-18-OH and 45 for PAF-18-OLi, respectively. The selectivity of PAF-18-OLi at 273 K is nearly four times higher than that of

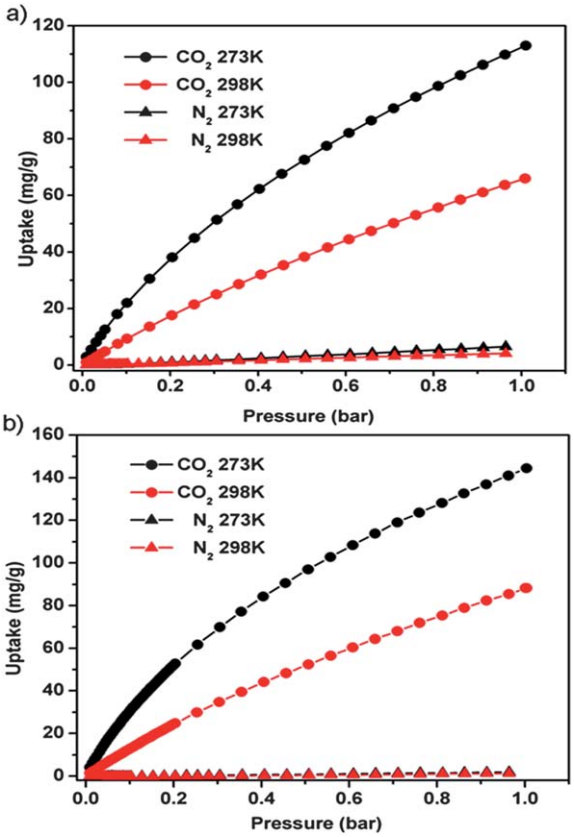

Fig. 4 The adsorption isotherms of CO_2 and N_2 at 273 K and at 298 K for PAF-18-OH (a) and PAF-18-OLi (b).

PAF-18-OH at the same conditions. The exceedingly high CO_2/N_2 selectivity of PAF-18-OLi could be attributed to the presence of the Li ions in the framework, which drastically enhance the adsorption of polar CO_2 molecules, and the decrease in the BET surface area and pore volume limits N_2 uptake.

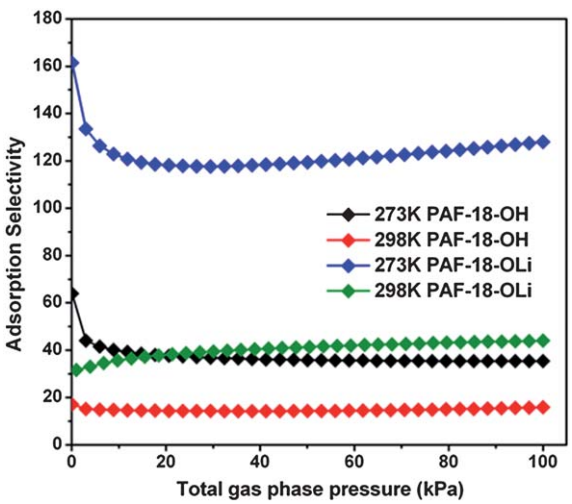

Fig. 5 IAST predicted 15% CO_2 over 85% N_2 adsorption selectivities for PAF-18-OH (black at 273 K and red at 298 K) and PAF-18-OLi (blue at 273 K and dark green at 298 K).

Furthermore, we have also studied the capture of CO_2 from low-pressure post-combustion flue gas mixtures with a CO_2 content of ~15%. The CO_2 uptake is carried out at 0.15 bar and the N_2 adsorption at 0.85 bar, which is more relevant to practical applications.

In this respect, the CO_2/N_2 selectivity in the flue gas is evaluated by the mass of CO_2 taken up at 0.15 bar divided by the mass of N_2 taken up at 0.85 bar. For example, at 298 K (ambient temperature), the CO_2/N_2 selectivity of PAF-18-OH is estimated to be 4.3 whereas a value of 15.6 is calculated for PAF-18-OLi (Table 2). The tremendous increase in CO_2/N_2 selectivity for PAF-18-OLi can be due to the high adsorption affinity of CO_2 toward available Li ion sites, with the simultaneous effect of a decline in the pore volume of PAF-18-OLi, which would greatly limit the nitrogen uptake in a gas mixture if CO_2 is pre-adsorbed at ambient temperature and pressure (Fig. S8†). It should be mentioned that the selectivity of CO_2 over N_2 is increased at low temperature (273 K, see Table 2), which is in good agreement with the IAST predicted result. The enhanced CO_2/N_2 selectivity after lithiation provides a new approach to develop new types of solid adsorbents for CO_2 capture and sequestration.

The H_2 adsorption for PAF-18-OH and PAF-18-OLi

In the current work, we have also studied the possibility of PAF-18-OH and PAF-18-OLi for H_2 storage. Fig. 6a shows hydrogen adsorption isotherms for both PAF materials at 77 K and 87 K. Based on the isotherms, the H_2 uptake of PAF-18-OH is calculated to be 1.35 wt% at 77 K, and 0.95 wt% at 87 K at 1 bar, respectively. After lithiation, the H_2 uptake has been significantly increased. The H_2 uptake of PAF-18-OLi increases with Li content in PAF-18-OLi (Fig. S7b†); when the Li content exceeds 4.2 wt%, the H_2 uptake decreases (Fig. S7b†).

PAF-18-OLi with a complete lithiation Li content of 4.2 wt% shows a maximum uptake of 1.65 wt% at 77 K, and 1.17 wt% at 87 K at 1 bar, respectively. Additionally, the Q_{st} is calculated from the H_2 adsorption data at 77 K and 87 K using the virial method (details in ESI†).[26] Fig. 6b shows that the Q_{st} of PAF-18-OLi is higher than that of PAF-18-OH. This suggests that the Li ions in PAF-18-OLi promote strong mutual interactions between hydrogen molecules and the PAF framework.

Table 2 Summary of the CO_2/N_2 selectivity for PAF-18-OH and PAF-18-OLi

Materials	273 K $S^{a}_{(CO_2/N_2)}$ [a]	298 K $S^{a}_{(CO_2/N_2)}$	273 K $S^{b}_{(CO_2/N_2)}$ [b]	298 K $S^{b}_{(CO_2/N_2)}$
PAF-18-OH	34	16	8.4	4.3
PAF-18-OLi	129	45	25	15.6

[a] $S^{a}_{(CO_2/N_2)}$ is calculated by the IAST model from 85% N_2 and 15% CO_2, 1 atm. [b] $S^{b}_{(CO_2/N_2)}$ is calculated by dividing the mass of CO_2 taken up at 0.15 bar by that of N_2 taken up at 0.85 bar.

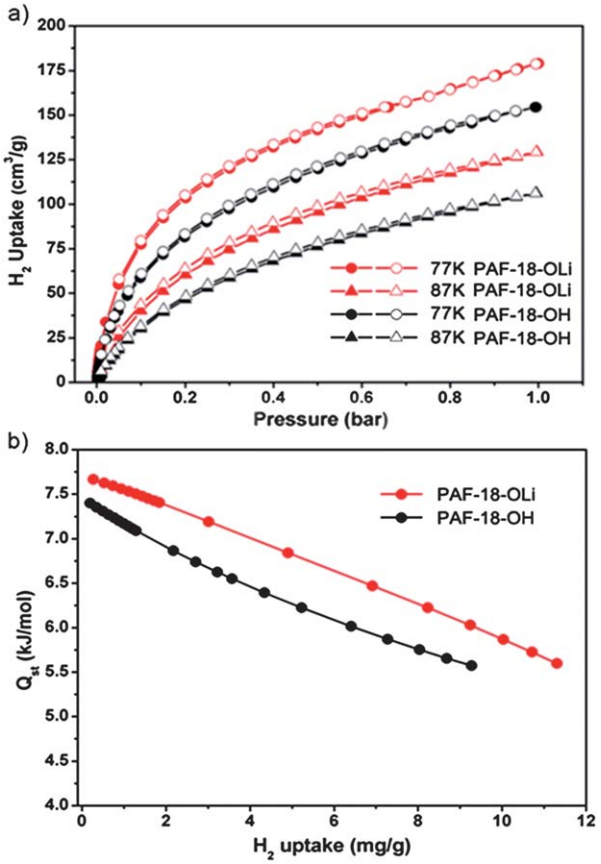

Fig. 6 (a) H_2 adsorption (solid symbols) and desorption (open symbols) isotherms of PAF-18-OH and PAF-18-OLi at 77 K and 87 K; (b) plots of H_2 adsorption Q_{st} of PAF-18-OH and PAF-18-OLi *versus* the H_2 uptake.

Conclusions

In conclusion, we have synthesized novel porous aromatic frameworks, PAF-18-OH and their lithiated derivative, PAF-18-OLi *via* a Sonogashira–Hagihara cross-coupling reaction. The tunability of the Li content in PAF-18-OLi shows different capacities for CO_2 and H_2 adsorption. The completely lithiated PAF-18-OLi exhibits the highest CO_2 and H_2 adsorption ability, which is due to stronger interactions of gas molecules with the lithium derived PAF framework. CO_2 capture from simulated flue gas is exemplified by PAF-18-OH and PAF-18-OLi. In the case of PAF-18-OLi, high CO_2/N_2 selectivity, up to 129, under ambient temperature and pressure is obtained, the value of which is almost four times higher than that of PAF-18-OH at the same conditions. Notably, the PAF-18-OLi material also exhibits high stability. The development of high-performance porous organic frameworks with remarkably high CO_2/N_2 selectivity, excellent sorption capacity of CO_2 and H_2, and high stability would pave the way for carbon dioxide capture and sequestration, and hydrogen storage.

Acknowledgements

We are grateful for the financial support of the National Basic Research Program of China (973 Program, grant no. 2012CB821700), Major International (Regional) Joint Research Project of NSFC (grant no.21120102034) and NSFC (grant no. 20831002).

Notes and references

1 IPCC, Summary for Policymakers, in: *Climate Change 2007: The Physical Science Basis*, Cambridge University Press, Cambridge, UK, 2007.

2 (*a*) S. Keskin, T. M. van Heest and D. S. Sholl, *ChemSusChem*, 2010, **3**, 879; (*b*) S. Chu, *Science*, 2009, **325**, 1599; (*c*) R. S. Haszeldine, *Science*, 2009, **325**, 1647; (*d*) J. Sculley, D. Yuan and H. C. Zhou, *Energy Environ. Sci.*, 2011, **4**, 2721.

3 (*a*) Y. S. Bae and R. Q. Snurr, *Angew. Chem., Int. Ed.*, 2011, **50**, 11586; (*b*) D. M. DAlessandro, B. Smit and J. R. Long, *Angew. Chem.*, 2010, **122**, 6194; *Angew. Chem., Int. Ed.*, 2010, **49**, 6058.

4 (*a*) L. Schlapbach and A. Züttel, *Nature*, 2001, **414**, 353; (*b*) U. Eberle, M. Felderhoff and F. Schüth, *Angew. Chem., Int. Ed.*, 2009, **48**, 6608; (*c*) V. V. Struzhkin, B. Militzer, W. L. Mao, H. Mao and R. J. Hemley, *Chem. Rev.*, 2007, **107**, 4133.

5 (*a*) X. Peng, W. C. Wang, R. S. Xue and Z. M. Shen, *AIChE J.*, 2006, **52**, 994; (*b*) M. B. Kim, Y. S. Bae, D. K. Choi and C. H. Lee, *Ind. Eng. Chem. Res.*, 2006, **45**, 5050; (*c*) V. Goetz, O. Pupier and A. Guillot, *Adsorption*, 2006, **12**, 55.

6 (*a*) S. Cavenati, C. A. Grande and A. E. Rodrigues, *J. Chem. Eng. Data*, 2004, **49**, 1095; (*b*) P. Y. Li and F. H. Tezel, *Microporous Mesoporous Mater.*, 2007, **98**, 94; (*c*) J. M. Leyssale, G. K. Papadopoulos and D. N. Theodorou, *J. Phys. Chem. B*, 2006, **110**, 22742; (*d*) R. Babarao, Z. Q. Hu, J. W. Jiang, S. Chempath and S. I. Sandler, *Langmuir*, 2007, **23**, 659.

7 (*a*) M. Eddaoudi, J. Kim, N. Rosi, D. Vodak, J. Wachter, M. O'Keeffe and O. M. Yaghi, *Science*, 2002, **295**, 469; (*b*) G. Férey, C. M. Draznieks, C. Serre, F. Millange, J. Dutour, S. Surblé and I. Margiolaki, *Science*, 2005, **309**, 2040; (*c*) J. S. Seo, D. Whang, H. Lee, S. I. Jun, J. Oh, Y. J. Jeon and K. Kim, *Nature*, 2000, **404**, 982; (*d*) D. M. D'Alessandro, B. Smit and J. R. Long, *Angew. Chem., Int. Ed.*, 2010, **49**, 6058; (*e*) B. Q. Ma, K. L. Mulfort and J. T. Hupp, *Inorg. Chem.*, 2005, **44**, 4912; (*f*) S. Kitagawa, R. Kitaura and S. Noro, *Angew. Chem., Int. Ed.*, 2004, **43**, 2334; (*g*) B. Zheng, J. Bai, J. Duan, L. Wojtas and M. J. Zaworotko, *J. Am. Chem. Soc.*, 2011, **133**, 748; (*h*) R. Luebke, J. F. Eubank, A. J. Cairns, Y. Belmabkhout, L. Wojtas and M. Eddaoudi, *Chem. Commun.*, 2012, **48**, 1455; (*i*) B. L. Chen, S. Q. Ma, F. Zapata, F. R. Fronczek, E. B. Lobkovsky and H. C. Zhou, *Inorg. Chem.*, 2007, **46**, 1233; (*j*) B. L. Chen, X. B. Zhao, A. Putkham, K. Hong, E. B. Lobkovsky, E. J. Hurtado, A. J. Fletcher and K. M. Thomas, *J. Am. Chem. Soc.*, 2008, **130**, 6411; (*k*) Q. R. Fang, G. S. Zhu, M. Xue, J. Y. Sun and S. L. Qiu, *Dalton Trans.*, 2006, 2399.

8 (*a*) J. X. Jiang, F. Su, A. Trewin, C. D. Wood, N. L. Campbell, H. Niu, C. Dickinson, A. Y. Ganin, M. J. Rosseinsky, Y. Z. Khimyak and A. I. Cooper, *Angew. Chem., Int. Ed.*,

2007, **46**, 8574; (*b*) M. P. Tsyurupa and V. A. Davankov, *React. Funct. Polym.*, 2002, **53**, 193.

9 (*a*) N. B. McKeown, P. M. Budd, K. J. Msayib, B. S. Ghanem, H. J. Kingston, C. E. Tattershall, S. Makhseed, K. J. Reynolds and D. Fritsch, *Chem.–Eur. J.*, 2005, **11**, 2610; (*b*) N. B. McKeown and P. M. Budd, *Chem. Soc. Rev.*, 2006, **35**, 675.

10 L. Chen, Y. Honsho, S. Seki and D. Jiang, *J. Am. Chem. Soc.*, 2010, **132**, 6742.

11 (*a*) T. Ben, H. Ren, S. Q. Ma, D. P. Cao, J. H. Lan, X. F. Jing, W. C. Wang, J. Xu, F. Deng, J. M. Simmons, S. L. Qiu and G. S. Zhu, *Angew. Chem., Int. Ed.*, 2009, **48**, 9457; (*b*) H. Ren, T. Ben, F. Sun, M. Guo, H. Ma, K. Cai, S. L. Qiu and G. S Zhu, *J. Mater. Chem.*, 2011, **21**, 10348; (*c*) H. Ren, T. Ben, E. S. Wang, X. F. Jing, M. Xue, B. B. Liu, Y. Cui, S. L. Qiu and G. S. Zhu, *Chem. Commun.*, 2010, **46**, 291; (*d*) W. Lu, D. Yuan, D. Zhao, C. I. Schilling, O. Plietzsch, T. Muller, S. Bräse, J. Guenther, J. Blümel, R. Krishna, Z. Li and H. C. Zhou, *Chem. Mater.*, 2010, **22**, 5964; (*e*) W. Wang, H. Ren, F. Sun, K. Cai, H. P. Ma, J. Du, H. Zhao and G. S. Zhu, *Dalton Trans.*, 2012, **41**, 3933; (*f*) X. Jing, F. Sun, H. Ren, Y. Tian, M. Guo, L. Li and G. S. Zhu, *Microporous Mesoporous Mater.*, 2013, **165**, 92; (*g*) Y. Yuan, F. Sun, H. Ren, X. Jing, W. Wang, H. Ma, H. Zhao and G. S. Zhu, *J. Mater. Chem.*, 2011, **21**, 13498; (*h*) F. Yuan, Y. Yan, Z. Ren, H. Liu, Q. Zhu and G. Sun, *F. Acta Chim. Sinica*, 2012, **70**, 1446.

12 (*a*) H. Furukawa and O. M. Yaghi, *J. Am. Chem. Soc.*, 2009, **131**, 8875; (*b*) A. P. Cote, A. I. Benin, N. W. Ockwig, M. O'Keeffe, A. J. Matzger and O. M. Yaghi, *Science*, 2005, **310**, 1166; (*c*) H. M. Kaderi, J. R. Hunt, J. L. Mendoza, A. P. Cote, R. E. Taylor, M. O'Keeffe and O. M. Yaghi, *Science*, 2007, **316**, 268.

13 P. Kuhn, M. Antonietti and A. Thomas, *Angew. Chem., Int. Ed.*, 2008, **47**, 3450.

14 (*a*) E. R. Thomas, T. J. Karl, S. Li, J. Puru and M. E. Hani, *J. Mater. Chem.*, 2011, **21**, 10629; (*b*) Y. H. Jin, B. A. Voss, R. D. Noble and W. Zhang, *Angew. Chem., Int. Ed.*, 2010, **49**, 6348; (*c*) R. Dawson, E. Stöckel, J. R. Holst, D. J. Adams and A. I. Cooper, *Energy Environ. Sci.*, 2011, **4**, 4239.

15 A. L. Chaffee, G. P. Knowles, Z. Liang, J. Zhany, P. Xiao and P. A. Webley, *Int. J. Greenhouse Gas Control*, 2007, **1**, 11.

16 D. Aaron and C. Tsouris, *Sep. Sci. Technol.*, 2005, **40**, 321.

17 (*a*) Y. S. Bae, A. M. Spokoyny, O. K. Farha, R. Q. Snurr, J. T. Hupp and C. A. Mirkin, *Chem. Commun.*, 2010, **46**, 3478; (*b*) Z. Q. Wang and S. M. Cohen, *Chem. Soc. Rev.*, 2009, **38**, 1315; (*c*) R. Dawson, D. J. Adams and A. I. Cooper, *Chem. Sci.*, 2011, **2**, 1173; (*d*) D. Himsl, D. Wallacher and M. Hartmann, *Angew. Chem.*, 2009, **121**, 4710; *Angew. Chem., Int. Ed.*, 2009, **48**, 4639.

18 (*a*) Y. J. Choi, J. W. Lee, J. H. Choi and J. K. Kang, *Appl. Phys. Lett.*, 2008, **92**, 173102; (*b*) J. Lan, D. Cao, W. Wang and B. Smit, *ACS Nano*, 2010, **4**, 4225; (*c*) A. Mavrandonakis, E. Tylianakis, A. K. Stubos and G. E. Froudakis, *J. Phys. Chem. C*, 2008, **112**, 7290; (*d*) A. Blomqvist, C. M. Araujo, P. Srepusharawoot and R. Ahuja, *Proc. Natl. Acad. Sci. U. S. A.*, 2007, **104**, 20173.

19 (*a*) K. L. Mulfort, O. K. Farha, C. L. Stern, A. A. Sarjeant and J. T. Hupp, *J. Am. Chem. Soc.*, 2009, **131**, 3866; (*b*) Z. Xiang, Z. Hu, D. Cao, W. Yang, J. Lu, B. Han and W. Wang, *Angew. Chem., Int. Ed.*, 2011, **50**, 491; (*c*) A. Li, R. Lu, Y. Wang, X. Wang, K. Han and W. Deng, *Angew. Chem., Int. Ed.*, 2010, **49**, 3330; (*d*) K. L. Mulfort and J. T. Hupp, *J. Am. Chem. Soc.*, 2007, **129**, 9604; (*e*) D. Himsl, D. Wallacher and M. Hartmann, *Angew. Chem., Int. Ed.*, 2009, **48**, 4639; (*f*) S. Yang, X. Lin, A. J. Blake, K. M. Thomas, P. Hubberstey, N. R. Champness and M. Schröder, *Chem. Commun.*, 2008, 6108; (*g*) K. L. Mulfort, T. M. Wilson, M. R. Wasielewski and J. T. Hupp, *Langmuir*, 2009, **25**, 503; (*h*) F. Nouar, J. Eckert, J. F. Eubank, P. Forster and M. Eddaoudi, *J. Am. Chem. Soc.*, 2009, **131**, 2864.

20 (*a*) W. Lu, D. Yuan, D. Zhao, I. S. Christine, O. Plietzsch, T. Muller, S. Bräse, J. Guenther, J. Blümel, R. Krishna, Z. Li and H. C. Zhou, *Chem. Mater.*, 2010, **22**, 5964; (*b*) E. Kiehlmann and R. W. Lauener, *Can. J. Chem.*, 1989, **67**, 335.

21 The palladium-catalyzed Sonogashira–Hagihara cross-coupling reaction is also known for the synthesis of conjugated microporous polymers (CMPs) reported by the group of Andrew I. Cooper. See: (*a*) R. Dawson, A. I. Cooper and D. J. Adams, *Prog. Polym. Sci.*, 2012, **37**, 530; (*b*) J. X. Jiang, F. Su, A. Trewin, C. D. Wood, H. Niu, J. T. A. Jones, Y. Z. Khimyak and A. I. Cooper, *J. Am. Chem. Soc.*, 2008, **130**, 7710; (*c*) J. X. Jiang, A. Trewin, F. Su, C. D. Wood, H. Niu, J. T. A. Jones, Y. Z. Khimyak and A. I. Cooper, *Macromolecules*, 2009, **42**, 2658; (*d*) R. Dawson, A. Laybourn, R. Clowes, Y. Z. Khimyak, D. J. Adams and A. I. Cooper, *Macromolecules*, 2009, **42**, 8809.

22 M. Inagaki and O. Tanaike, *Synth. Met.*, 1995, **73**, 77.

23 J. P. Contour, A. Salesse, M. Froment, M. Garreau, J. Thevenin and D. Warin, *J. Microsc. Spectrosc. Electron.*, 1979, **4**, 483.

24 R. Dawson, A. Laybourn, Y. Z. Khimyak, D. J. Adams and A. I. Cooper, *Macromolecules*, 2010, **43**, 8524.

25 (*a*) W. Lu, D. Yuan, J. Sculley, D. Zhao, R. Krishna and H. C. Zhou, *J. Am. Chem. Soc.*, 2011, **133**, 18126; (*b*) E. D. Bloch, D. Britt, C. Lee, C. J. Doonan, F. J. Uribe-Romo, H. Furukawa, J. R. Long and O. M. Yaghi, *J. Am. Chem. Soc.*, 2010, **132**, 14382.

26 (*a*) R. C. Lochan and M. Head-Gordon, *Phys. Chem. Chem. Phys.*, 2006, **8**, 1357; (*b*) S. K. Bhatia and A. L. Myers, *Langmuir*, 2006, **22**, 1688.

27 Q. Xu, D. H. Liu, Q. Y. Yang, C. L. Zhong and J. G. Mi, *J. Mater. Chem.*, 2010, **20**, 706.

28 (*a*) Y. S. Bae, A. M. Spokoyny, O. K. Farha, R. Q. Snurr, J. T. Hupp and C. A. Mirkin, *Chem. Commun.*, 2010, **46**, 3478; (*b*) Y. J. Choi, J. W. Lee, J. H. Choi and J. K. Kang, *Appl. Phys. Lett.*, 2008, **92**, 173102; (*c*) R. Dawson, D. J. Adams and A. I. Cooper, *Chem. Sci.*, 2011, **2**, 1173; (*d*) A. Mavrandonakis, E. Tylianakis, A. K. Stubos and G. E. Froudakis, *J. Phys. Chem. C*, 2008, **112**, 7290.

